Journal of Thermal Analysis and Calorimetry, Vol. 60 (2000) 641–658

KINETIC ANALYSIS USING MULTIVARIATE NON-LINEAR REGRESSION I. Basic concepts*

J. Opfermann

NETZSCH-Gerätebau GmbH, Wittelsbacherstraße 42, D-95100 Selb, Germany

(Received July 13, 1998; in revised form July 20, 1999)

Abstract

In principle, the kinetic analysis of thermal effects has limitations when based on a single measurement. Using a simulated example and the dehydration of $Ca(OH)_2$, it will be shown that, through the simultaneous application of non-linear regression to several measurements run at different heating rates (multivariate non-linear regression), the difficult problem of determining the probable reaction type can be reliably solved.

Keywords: $Ca(OH)_2$, multiple-step kinetics, multivariate non-linear regression

Introduction

The application of kinetic analysis will be considered from two aspects:

- From the scientific aspect, an attempt is made to record the individual steps of the entire process as a model, to clarify them and interpret them in a physical/chemical sense.
- From the technical aspect, the kinetic analysis is examined as a tool for data reduction. The information is extracted from a series of measurements with many data points in the form of a model with few parameters.
  This model is then used in the preparation of predictions and for process optimization.

Considering the application of kinetic analysis from these two aspects requires a different procedure:

A model (hypothesis) is set up, in which the individual reaction steps can be interpreted chemically and/or physically. The hypothesis is compared with the experimental results and, if possible, with results obtained from other experimental methods as well. If the hypothesis and experiment are contradictory, the hypothesis is replaced with another. If they agree, further experiments can be carried out in order to further support or refine the hypothesis [1]. In many cases, the tests involve variation

* II. Simulation of two-step reactions [32]

1418–2874/2000/ $ 5.00

Akadémiai Kiadó, Budapest
Kluwer Academic Publishers, Dordrecht

of the test sample, so as to make its specific properties apparent. Such a procedure for thermoanalytical measurements is demonstrated by Flammersheim *et al.* [2].

From scientific aspect, the analysis of the reaction kinetics should therefore answer three questions:

1. How does one investigate the mechanism of the gross reaction?
2. How does one calculate the reaction conversion as a function of time?
3. How can one make the course of an elementary reaction understandable with molecular models?

From technical aspect, one usually starts with a given test sample. A targeted variation of this sample is often impossible since, for example, the supplier of the material does not want to reveal his know-how. The kinetic model is, to the greatest extent, formal. Therefore, the reactants are also formal; their concentrations assume only values between 0 and 1.

The kinetic model as a combination of individual steps serves as an efficient filter for data reduction. An interpretation of the single steps and their parameters is not planned for the time being [3].

Often, the behavior of the test sample is investigated under conditions as close as possible to those for which the predictions will be made. In contrast, the effects of specific conditions [4] are only seldom taken into consideration. The simpliest model to be designed should be capable of describing the essential characteristics of the data in the reaction field over the time and temperature of the measurements.

General statistical knowledge says that the level of confidence of predictions in the range of analysis is especially high and is directly proportional to the quality of the fit. For thermoanalytical measurements, this means that the largest possible range of the accessible time/temperature field [5] must be covered with isothermal measurements at different temperatures or with dynamic measurements at different heating rates.

In their practical realization, the two aspects have much in common, in spite of their antithetic goals:

- A kinetic model must be set up.
  The kinetic model contains, on the one hand, the reaction diagram, i.e. the combination of single reaction steps, and on the other hand, the concrete assignment of each reaction step to a reaction type.
- The parameters of the model must be specified so that the experiment may be described as well as possible.
- The aim is a comprehensive solution, which is valid for a greater range of the test parameters.

The basic concept

For kinetic analysis of the reaction (1), Eq. (2) is generally assumed.

$$A(s) \rightarrow B(s) + B'(g) \quad (1)$$

$$de/dt = -U(t,T,e,p) \quad (2)$$

where:

t/s	time,
T/K	temperature,
e	start concentration of the reactant,
p	concentration of the final product.

With the help of that, formalisms of homogeneous kinetics are applied to heterogeneous reactions [6]. From the scientific aspect, there are justified objections to this procedure, but not for the technical aspect described above.

It is further assumed that the conversion function, $U(t,T,e,p)$, can be described by two separable functions, $k(T)$ and $f(e,p)$:

$$U(t,T,e,p)=k(T(t))f(e,p) \tag{3}$$

For one-step reactions, $f(e,p)$ reduces to the known form, $f(x)$, where $e=1-\alpha$ and $p=\alpha$ (α=degree of conversion). The complete separation of variables in Eq. (3) is, however, only possible for one-step processes. Thus, an analytical solution of the differential Eq. (2) can also only be achieved for one-step reactions. For complex, multi-step processes, the differential Eq. (2) becomes a system of differential equations, for which a separation of variables is no longer possible. Therefore, there is no analytical solution either.

Indeed, Eqs (4a) and (4b) are suggested from the collision theory and the theory of the transition state, respectively. Since the term, T^m (m=1/2 or m=1), becomes noticeable in both equations, but only at low temperatures, m=0 and the Arrhenius Eq. (4) will be assumed to be valid for the following:

$$k(T)=A\exp(-E/RT) \tag{4}$$

$$k(T)=BT^{1/2}\exp(-E/RT) \tag{4a}$$

$$k(T)=CT\exp(-E/RT) \tag{4b}$$

Furthermore, it will be assumed that all reactions are irreversible. Accordingly, in carrying out the tests, the researcher must see that this condition is fulfilled to the greatest extent possible. For decomposition reactions, for example, the gaseous reaction products must be removed from the reaction chamber by applying vacuum or purging with gas.

A series of reaction types is listed in Table 1. This list contains classic homogeneous reactions and typical solids reactions. In comparison to the known reaction types [7], the list is extended with the combined autocatalytic types C1 and Cn, which, on careful examination, already represent parallel reactions with the same activation energy.

The above-stated requirement, for the most comprehensive validity possible of the solution found, is solved in a series of papers [8–10], in that first of all each measurement in a series of measurements is individually analyzed and only one-step reaction processes are considered. Only in a second step is a compromise solution sought by averaging the calculated kinetic parameters.

Table 1 Reaction types and corresponding reaction equations $de/dt = -A\exp(E/RT)f(e,p)$, e=start concentration of the reactant, p=concentration of the final product

Code	$f(e,p)$	Reaction type
F1	e	first-order reaction
F2	e^2	second-order reaction
Fn	e^n	n^{th}-order reaction
R2	$2e^{1/2}$	two-dimensional phase boundary reaction
R3	$3e^{2/3}$	three-dimensional phase boundary reaction
D1	$0.5/(1-e)$	one-dimensional diffusion
D2	$-1/\ln(e)$	two-dimensional diffusion
D3	$1.5e^{1/3}/(e^{-1/3}-1)$	three-dimensionsl diffusion (Jander's type)
D4	$1.5/(e^{-1/3}-1)$	three-dimensional diffusion (Ginstling–Brounstein type)
B1	ep	simple Prout–Tompkins equation
Bna	$e^n p^a$	expanded Prout–Tompkins equation (na)
C1–X	e(1+KcatX)	first-order reaction with autocatalysis through the reactants, X X = a product in the complex model, frequently X=p
Cn–X	e^n(1+KcatX)	n^{th}-order reaction with autocatalysis through the reactants, X
A2	$2e(-\ln(e))^{1/2}$	two-dimensional nucleation
A3	$3e(-\ln(e))^{2/3}$	three-dimensional nucleation
An	$ne(-\ln(e))^{(n-1)/n}$	n-dimensional nucleation/nucleus growth according to Avrami-Erofeev

With multivariate kinetic analysis [5, 11–14], a totally different approach is taken: the assumption is made that the parameters of the model are *a priori* identical for all measurements. This is constrained by the determination of the parameters in an analysis of all of the measurements together. If the quality of fit is insufficient with the given model, the model must be improved through extension to multi-step reaction processes with different combinations. This is demonstrated in section 4 using the dehydration of $Ca(OH)_2$ as an example.

The kinetic parameters through which the model is characterized are divided into two groups. One group is valid for all scans and is therefore model-specific. The other group is specific for one scan at a time. For example, for the description of a two-step secondary reaction A → B → C one obtains the set of parameters given in Table 2 from three thermogravimetric measurements. Here, only parameters 8 through 10 are scan-specific, all other parameters are model-specific and are thus valid for all scans. The parameters are determined via a hybrid regularized Gauss–Newton method (Marquardt method). Related details can be found in Appendix 1.

Table 2 Relationship between the parameters and the reaction pattern for a two-step consecutive reaction A→ B→C and the assumption of n^{th}-order reactions and three thermogravimetric measurements

#	Parameter	Definition
		Step 1: A→B
1	lg($A1$/s^{-1})	logarithm of the pre-exponential factor of step 1
2	$E1$/kJ mol^{-1}	activation energy of step 1
3	$n1$	order of reaction of step 1 Step 2: B→C
4	lg($A2$/s^{-1})	logarithm of the pre-exponential factor of step 2
5	$E2$/kJ mol^{-1}	activation energy of step 2
6	$n2$	order of reaction of step 2
7	FollReact. 1	share of step 1 in the total mass loss (the share of step 2 is 1 – FollReact. 1)
8	MassDiff 1%	total mass loss of scan 1
9	MassDiff 2%	total mass loss of scan 2
10	MassDiff 3%	total mass loss of scan 3

Improvement of the distinguishability of different reaction types through multi-curve analysis

A single dynamic measurement already contains all the information about the kinetic model and its parameters, but this information is generally insufficient to solve the above-stated problem satisfactorily [15–17]. A complaint was also made in more recent work, namely it is not possible to determine the reaction type with statistical cer-

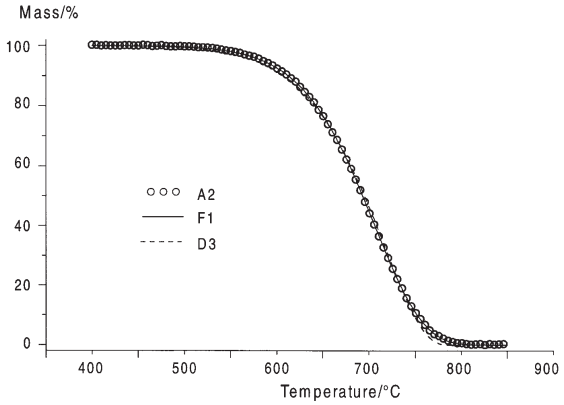

Fig. 1 Fit of a single TG measurement, simulated with reaction type A2 and a heating rate of 10 K min^{-1} to reaction types F1 and D3. Initial parameters for A2: lg(A/s^{-1})=1.079, E/kJ mol^{-1}=76.00

tainty when the temperature program is linear. Brown [18] is not totally unjustified in characterizing the previous procedure as 'steps in a minefield'.

Criado *et al*. [19] explain a simulated example in which a single TG curve, measured with the heating rate of 10 K min^{-1}, for which the reaction type is based on the two-dimensional nucleation reaction (A2), can be fitted almost congruently both with a first-order decomposition reaction (F1) and a three-dimensional Jander's-type diffusion (D3) (Fig. 1). This simply means that locally, i.e. for a single heating rate, several equivalent solutions exist and, therefore, no statistically certain decision is possible as to which reaction type applies. In the following, the kinetic data given in [19] will be used to simulate and analyze TG curves at different heating rates. In order to make realistic statements, the simulations are superposed with statistical noise (an amplitude of 0.2% of the maximum value).

The results shown in Table 3 are obtained with the additional heating rates of 1, 2.5 and 5 K min^{-1}. For reaction types A2, F1 and D3, a high quality of fit is always obtained for all heating rates (correlation coefficient>0.9995). Therefore, a specific local solution is found for each heating rate and each reaction type. The great differences in both the activation energies and the pre-exponential factors for the various reaction types are, however, remarkable. For that reason, it is not surprising that predictions based on the kinetic analysis of a single measurement generally lead to large deviations as compared to experiments with varied conditions.

Table 3 Kinetic parameters resulting from single-curve analyses with reaction types F1 and D3 from TG measurements, simulated with reaction type A2

Heating rate/ K min^{-1}	Reaction type	$lg(A/s^{-1})$	E/kJ mol^{-1}	Corr. coeff.
10.0	F1	6.06±0.02	168.7±0.3	0.999 995
	D3	12.13±0.18	306.1±3.3	0.999 719
5.0	F1	6.42±0.03	169.6±0.5	0.999 992
	D3	12.95±0.21	307.4±3.7	0.999 685
2.5	F1	6.83±0.04	171.4±0.7	0.999 989
	D3	13.88±0.24	310.4±4.1	0.999 672
1.0	F1	7.03±0.03	167.9±0.3	0.999 994
	D3	14.49±0.22	303.4±3.4	0.999 727

In contrast, if a comparison is made of the analysis of results for different heating rates but the same reaction type, the differences with respect to the activation energy are slight. This leads to the following conclusion: for the analysis of a single curve, even if there is practically no change in the activation energy when the heating rate is changed, this is not a sure indication that the correct reaction type has been determined. Taking the mean of the kinetic parameters from single curve analyses of measurements run at different heating rates [8] should also be viewed with caution.

Therefore, as a solution to the problem, Criado *et al.* [19] suggest running the measurement in the CRTA mode (controlled rate thermal analysis). With this special

temperature program, the mass decreases at a constant rate. By plotting the temperature with respect to the degree of conversion, one obtains specific curve profiles:

- monotonously rising for phase boundary reactions (R2, R3) and chemical reactions (F1, Fn),
- monotonously descending for one-dimensional diffusion (D1),
- sigmoidally rising for two- and three-dimensional diffusion (D2, D3, D4),
- through-shaped with defined dependence of the minimum on the reaction type (A2 through A4).

Based on the form, it is easier to identify the group to which the curve belongs. An important requirement for the applicability of this method is, however, the guaranteed presence of a one-step reaction.

With multivariate non-linear regression as the method of analysis, a different procedure is favored: several dynamic measurements run at different heating rates and/or several isothermal measurements run at different temperatures are brought together during the analysis.

For the example given above, a satisfactory fit is possible only with model A2 for the common analysis of the TG measurements run at heating rates of 1, 2.5, 5 and 10 K min^{-1} (Table 4 and Figs 2–4). This solution is then globally valid, at least for the range of heating rates between 1 and 10 K min^{-1}. Even for the non-applicable reaction types, the calculated activation energy now clearly lies closer to the value of 76 kJ mol^{-1} (Fig. 1), upon which the simulations are based. The position of the individual TG curves with respect to one another apparently forces the activation energy closer to the correct value, while the other kinetic parameters are optimized to achieve a high quality of fit. Compared to the single curve analysis, the quality of fit diminishes considerably for the non-applicable reaction types F1 and D3. That is also the reason why the distinguishability between the individual reaction types with an F-Test (Table 4) improves so drastically. (A detailed description of the F-Test can be found in Appendix 2.) Now the 'correct' reaction type is significantly recognized and the kinetic parameters apply.

Table 4 Kinetic parameters resulting from multiple-curve analyses (heating rates 1, 2.5, 5 and 10 K min^{-1}) with reaction types F1 and D3 from TG measurement, simulated with reaction type A2 and a noise level of 0.2%

Reaction type	$lg(A/s^{-1})$	E/kJ mol^{-1}	Corr. coeff.	F_{exp}	$F_{crit(0.05)}$
A2	1.079	76.0	0. 999 99	1.00	1.09
F1	2.406	98.7	0.980 89	5015	1.09
D3	4.196	148.7	0.943 02	14608	1.09

As investigations of the behavior, conducted using several measurements run at the same heating rate [20], have shown, the local solution is more stable for such a procedure, since the errors of measurement balance out. However, an increase in the distinguishability, as found when using measurements run at different heating rates, is not achieved.

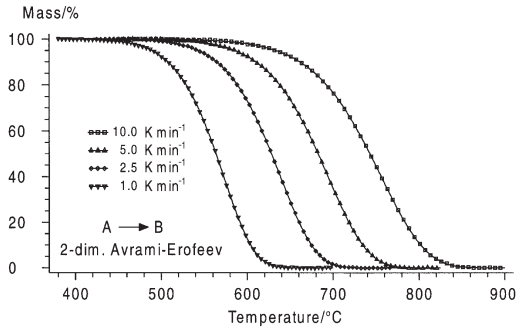

Fig. 2 Fit of TG measurements, simulated with reaction type A2 and a noise level of 0.2% for the heating rates 1, 2.5, 5 and 10 K min^{-1}, to reaction type A2. Signs measured, — calculated

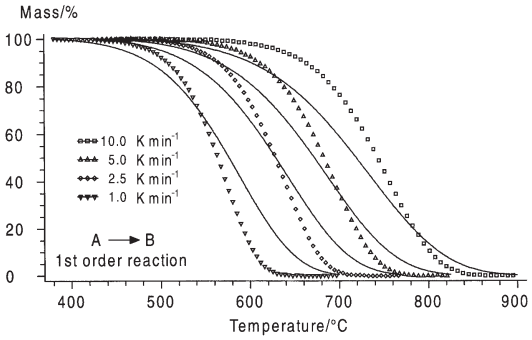

Fig. 3 Fit of TG measurements, simulated with reaction type A2 and a noise level of 0.2% for the heating rates 1, 2.5, 5 and 10 K min^{-1}, to reaction type F1. Signs measured, — calculated

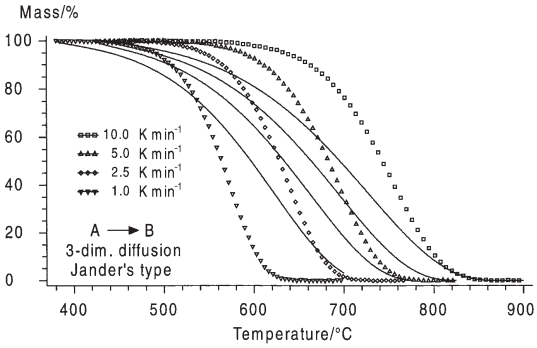

Fig. 4 Fit of TG measurements, simulated with reaction type A2 and a noise level of 0.2% for the heating rates 1, 2, 5 and 10 K min^{-1}, to reaction type D3. Signs measured, — calculated

Finding the probable model for actual measurements, illustrated by using the thermal decomposition of $Ca(OH)_2$ as an example

The objection could be made that, with simulated data, the situation is too favorable as compared to actual measurements and only for that reason is the distinguishability achieved. The thermal decomposition of $Ca(OH)_2$ will be used to show that, in spite of ever-present measurement errors, the multivariate data analysis leads to success.

Experimental

The thermogravimetric measurements were carried out on a NETZSCH STA 429 under N_2 and a low partial pressure of H_2O at heating rates of 5, 10.3 and 21 K min^{-1}. The sample masses were between 47 and 51 mg.

Single curve analysis

Figure 5 depicts the results of the kinetic analysis for a heating rate of 10.3 K min^{-1}. As with the simulations, the kinetic analysis for several reaction types provides an excellent quality of fit. This means that no decision can be made regarding the probable reaction type by means of an F-Test (Table 5). All of these solutions apply from the standpoint of the curve fit, though only locally – for the heating rate of 10 K min^{-1}. For other heating rates, other values are obtained for the kinetic parameters and, if necessary, another reaction type may give the best fit.

Table 5 Result of single-curve analyses of the thermal decomposition of $Ca(OH)_2$ with reaction types D4, D2, R2 and D3

Heating rate/ K min^{-1}	Reaction type	lg(A/s^{-1})	E/kJ mol^{-1}	Corr. coeff.	F_{exp}	$F_{crit(0.05)}$
21.5	D4	13.80	246.4	0.999 90	1.00	1.18
	D2	13.46	233.0	0.999 90	1.03	1.18
	R2	5.79	121.0	0.999 81	1.83	1.18
	R3	6.32	130.3	0.999 39	5.96	1.18
	D3	15.65	271.6	0.999 35	6.32	1.18
10.3	D4	15.20	262.1	0.999 95	1.00	1.19
	D2	14.78	248.0	0.999 93	1.50	1.19
	R2	6.29	128.0	0.999 87	2.64	1.19
	D3	17.31	290.0	0.999 50	10.02	1.19
	R3	6.93	138.6	0.999 47	10.44	1.19
5.0	D2	15.19	249.8	0.999 96	1.00	1.20
	D4	15.64	263.9	0.999 92	2.09	1.20
	R2	6.33	128.6	0.999 78	5.85	1.20
	D3	17.82	292.0	0.999 39	15.89	1.20
	R3	7.00	139.2	0.999 32	17.74	1.20

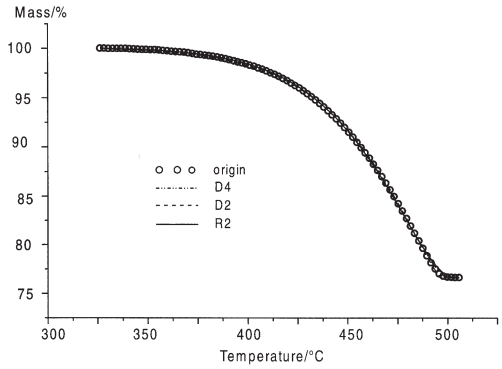

Fig. 5 Fit of a single TG measurement of the decomposition of $Ca(OH)_2$, to reaction types D4, D2 and R2. Heating rate: 10.3 K min^{-1}

Multiple curve analysis

The strength of multivariate data analysis becomes apparent in Figs 6 and 7 and Table 6. Indeed, the simultaneous kinetic analysis of all three heating rates shows that neither the three-dimensional diffusion (D4) nor the two-dimensional diffusion (D2), which most frequently led to the best fit for the single curve analysis, is the probable reaction type. Rather, it is the two-dimensional phase boundary reaction (R2), which was identified after having been ruled out as an acceptable model for the quality of fit in the single curve analysis for all heating rates.

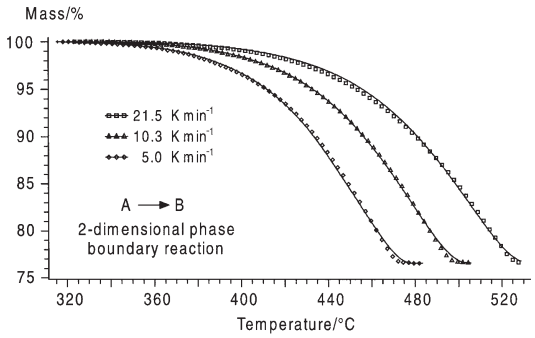

Fig. 6 Kinetic analysis of TG measurements on $Ca(OH)_2$ with reaction type R2. Signs measured, — calculated

The decision in favor or the two-dimensional phase boundary reaction is of great statistical significance in the multiple curve analysis (Table 6).

The question remains as to why the two-dimensional phase boundary reaction is characterized as an unacceptable reaction type in the single curve analysis. An initial answer to this question is provided by the model-free estimation of the activation energy as described by Ozawa, Flynn and Wall [21–23, details in Appendix 3] (Figs 8 and 9).

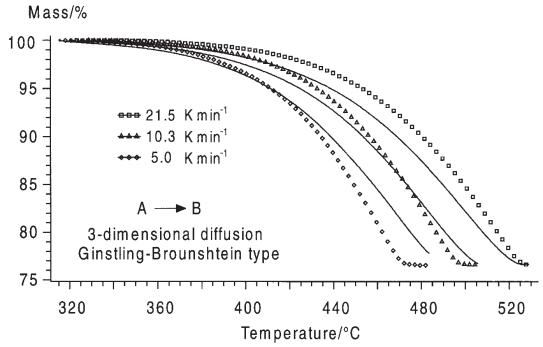

Fig. 7 Kinetic analysis of TG measurements on $Ca(OH)_2$ with reaction type D4. Signs measured, — calculated

Table 6 Result of multiple-curve analyses of the thermal decomposition of $Ca(OH)_2$, measured with heating rates of 5, 10.3 and 21.5 K min^{-1}

Reaction type	$lg(A/s^{-1})$	E/kJ mol^{-1}	Corr. coeff.	F_{exp}	$F_{crit(0.05)}$
R2	6.23	127.2	0.999 72	1.00	1.11
R3	6.49	132.6	0.999 19	2.88	1.11
D2	11.39	209.2	0.984 71	54.14	1.11
D4	11.29	199.5	0.982 96	60.28	1.11
D3	12.86	228.2	0.979 39	72.79	1.11

It is clear in Fig. 9, that the activation energy assumes a value of 160 kJ mol^{-1} at the beginning of the decomposition reaction and, with increasing mass loss, drops to a value of 125 kJ mol^{-1}. This dependence of the activation energy is an indication that the overall reaction contains at least two steps. Presumably, the type R2 main reaction, with an activation energy of 125 kJ mol^{-1}, is preceded by another reaction with a higher activation energy.

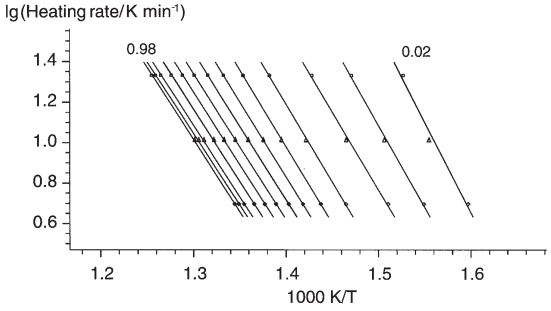

Fig. 8 Ozawa–Flynn–Wall model-free analysis of TG measurements on $Ca(OH)_2$. 0.02 and 0.98 are the degrees of reaction for the first and the last isoconversional line, respectively

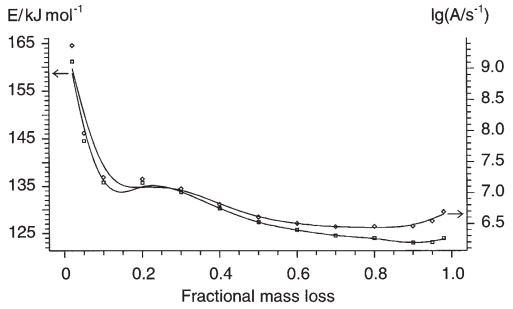

Fig. 9 Activation energy *vs.* fractional mass loss for TG measurements on $Ca(OH)_2$. □ – activation energy, ◊ – $\lg(A/s^{-1})$

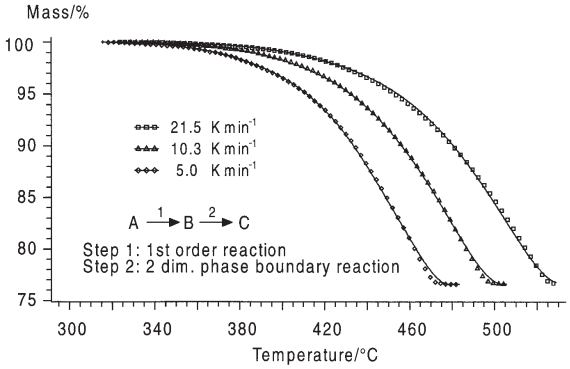

Fig. 10 Kinetic analysis of TG measurements on $Ca(OH)_2$, fitted as a two-step consecutive reaction with reaction types F1 and R2. Signs measured, — calculated

Table 7 Comparison of the results of multiple-curve analyses of the thermal decomposition of $Ca(OH)_2$ with one- and multiple-step reaction patterns

Reaction type(s)	Parameter	Value	Corr. coeff.	F_{exp}	$F_{crit(0.05)}$
F1	$\lg(A1/s^{-1})$	9.95±0.32	0.999 81	1.00	1.11
	$E1$/kJ mol^{-1}	151.4±4.5			
R2	$\lg(A2/s^{-1})$	6.35±0.03			
	$E2$/kJ mol^{-1}	128.8±0.4			
	FollReact.1	0.033±0.005			
R2	$\lg(A1/s^{-1})$	6.23±0.03	0.999 72	1.44	1.11
	$E1$/kJ mol^{-1}	127.2±0.3			
R3	$\lg(A1/s^{-1})$	6.49±0.05	0.999 19	4.15	1.11
	$E1$/kJ mol^{-1}	132.6±0.7			
D2	$\lg(A1/s^{-1})$	11.39±0.16	0.984 71	77.99	1.11
	$E1$/kJ mol^{-1}	209.2±2.3			

This presumption is confirmed by the kinetic analysis (Fig. 10, Table 7). The main reaction, characterized by a two-dimensional phase boundary reaction, is preceded by a first-order (F1) reaction. However, the first step amounts to only 3.3±0.5% of the total mass loss and is therefore not so obvious.

Conclusions

The difficulties of kinetic analysis, which are closely related to the high correlation of the kinetic parameters, are actually rooted in the meager amount of information contained in a single measurement [24]. Therefore, in spite of a high quality of fit (correlation coefficient >0.999), the kinetic parameters also have a relatively high confidence interval [15]. Through multiple curve analysis (multivariate analysis), with which several measurements run at different heating rates and/or isothermal measurements run at different temperatures are combined in one analysis, the behavior of the sample is examined in a global range of the reaction field (Fig. 11). While in isothermal measurements with one curve already the reaction type can be estimated and only with additional curves the activation energy, on the base of one dynamic measurement both, reaction type and activation energy, are estimable. But the confidence of such an estimation is very small. In a single curve analysis only the information nearly to the temperature line is taken into account, i.e. the temperature line with a heating rate of 20 K min^{-1}. Contrary to this, in multiple curve analysis the information of any curve is not handled separately, but in the context to the information of all curves, which are summarized in this analysis.

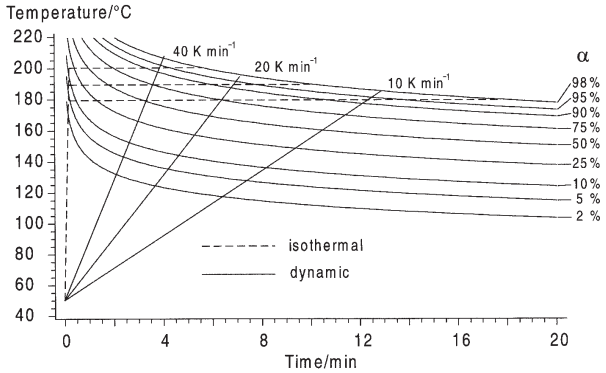

Fig. 11 Plot of the reaction field through isothermal and dynamic measurements (schematic). It demonstrates the different behavior of isothermal and dynamic measurements: isothermal measurements start with a strong, dynamic measurements with a soft variation in α. The set of isothermal as well as of dynamic measurements contains information of the area between the temperature lines

With the greater amount of information now available as compared to a single curve, the desired improvement in distinguishability between reaction types is achieved.

Undoubtedly, isothermal measurements have the advantage that there is a complete separation of the variables time and temperature. Frequently, however, detection of the transition from rapid heating to isothermal operation is problematic. If autocatalytically activated reactions are disregarded, the highest conversion lies directly in this range. In contrast, dynamic measurements have the decisive advantage that they are experimentally easier to perform. In addition, only this type of measurement is reasonable for instruments with slower furnaces.

Previous experience speaks for a variation of the heating rate by a factor of at least 5. Three to four measurements are generally sufficient. For complex problems, both the range of heating rates and the number of measurements should be increased if necessary. It should be emphasized, that only the comparison of measurements run at different heating rates makes the presence of competing reactions discernible [32].

Overall, multivariate analysis – with its improved power of discernment – proves to be the way to achieve a kinetic model that is valid for a greater time and temperature range. Only now do predictions – isothermal or for a specific temperature program –, that are so important to technology, attain the required level of confidence. At the same time, one of the requirements is fulfilled for tackling the next stage in the kinetic analysis of thermal effects, namely the analysis of multiple step reaction paths.

Appendix 1

The task of non-linear regression is the iterative calculation of the minimum sum of least squares, LSQ. According to the maximum likelihood theorem, the method is optimal when the weighting Eq. (6) is carried out at the same time. Then, LSQ yields χ^2 [25].

$$\mathrm{LSQ}=\sum_{j=1}^{M}\sum_{k=\mathrm{Start}_j i}^{\mathrm{Final}_j} w_{j,k}(\mathrm{Yexp}_{j,k}-\mathrm{Ycal}_{j,k})^2 \tag{5}$$

where

$$w_{j,k}=\frac{\sum_{j=1}^{M}(\mathrm{Final}_j-\mathrm{Start}_j)}{M(\mathrm{Final}_j-\mathrm{Start}_j)}\frac{1}{S^2(\mathrm{Yexp}_{j,k})+S^2(\mathrm{Ycal}_{j,k})} \tag{6}$$

and

M	the number of measurements,
j	curve index,
Start_j	index of the point for which $x \geq x_{\mathrm{Start}}$ is valid, (x_{Start} is preset by the user)
Final_j	index of the point for which $x \leq x_{\mathrm{final}}$ is valid, (x_{final} is preset by the user)
$\mathrm{Yexp}_{j,k}$	experimental value of the curve j in points k,
$\mathrm{Ycal}_{j,k}$	calculated value for the point j, k,
$S^2(\mathrm{Yexp}_{j,k})$	the experimental error of the measured point j, k,
$S^2(\mathrm{Ycal}_{j,k})$	the error of the calculated point j, k.

Through the first term in Eq. (6), each measurement enters into LSQ with the same weight, independent from its number of points, N_j. For the second term in Eq. (6), it is generally assumed that $S^2(Yexp_{j,k})$ is independent of the heating rate and $S^2(Yexp_{j,k}) >> S^2(Ycal_{j,k})$ applies. This term is therefore normally set equal to 1. More recent experience [26] has now shown that, specifically for DSC measurements, this first assumption is not correct. Apparently the points from measurements run at lower heating rates exhibit a smaller absolute error than measurements run at higher heating rates. Therefore, a weighting for which Eqs(7a) or (7b) applies appears to be better. More experience is required in this area.

$$w_{j,k}=\frac{\sum_{i=1}^{M}(Final_i-Start_i)}{M(Final_j-Start_j)}\frac{1}{abs(Max(Yexp_{j,k}))+abs(Min(Yexp_{j,k}))} \tag{7a}$$

$$w_{j,k}=\frac{\sum_{j=1}^{M}(Final_i-Start_i)}{M(Final_j-Start_j)}\frac{1}{Max(Y^2exp_{j,k})+Min(Y^2exp_{j,k})} \tag{7b}$$

$Ycal_{j,k}$ is the solution for the system of differential equations. For the example shown, a two-step consecutive reaction A → B → C, one obtains

$$\frac{da}{dt}=-f(a,b)A1\exp\left(-\frac{E1}{RT_{j,k}}\right) \tag{8}$$

$$\frac{db}{dt}=-\frac{da}{dt}-f(b,c)A2\exp\left(-\frac{E2}{RT_{j,k}}\right) \tag{9}$$

$$c=1-a-b \tag{10}$$

Between the interpolation nodes, the temperature $T_{j,k}$ is interpolated linearly. $Ycal_{j,k}$ then results under consideration of the balance equation for thermogravimetric measurements Eq. (11) or for DSC measurements Eq. (12). Here, the theoretical concentrations a, b and c have the following initial values: a_0=0.99950, b_0=0.00049 and c_0=0.00001.

For the solution of the system of differential equations, a 5th-degree Runge–Kutta matrix method (Prince–Dormand method [27]) is employed as a subprogram. This subprogram is, for its part, tied into a hybrid regularized Gauss–Newton method [28]. Further details can be found in [29].

$$Ycal_{j,k}=Ycal_{j,0}+MassDiff_j[FollReact1(1-a)+(1-FollReact1)c] \tag{11}$$

$$Ycal_{j,k}=Area_j[FollReact1\frac{da}{dt}+(1-FollReact1)\frac{dc}{dt}] \tag{12}$$

Appendix 2

For the F-Test, two variances, V_1 and V_2, are related ($V_2>V_1$) and compared with the statistical quantile, $F_{crit}(\alpha, f_1, f_2)$, where α is the given confidence level (or level of error probability) and f_1 and f_2 are the degrees of freedom for the variances, V_1 and V_2. $F_{crit}(\alpha, f_1, f_2)$ is calculated using a precise approximation equation [30].

$$F_{exp}=\frac{V_2}{V_1} \tag{13}$$

where

$$V_j=LSQ_j/f_j \tag{14}$$

Now if $F_{exp} > F_{crit}$, model 1 with the variance, V_1, is significantly better suited for the characterization of the given measurement than model 2 with the variance, V_2. In the strictest sense, the F-Test has only been realized for linear problems [31]. Nevertheless, for lack of a better test criterion, it is used for nonlinear problems.

An additional step is tested for significance in a similar way [31]. Model 1 should have n reaction steps with LSQ_1 and the degree of freedom, f_1. For model 2, which should have one additional reaction step, LSQ_2 and the degree of freedom, f_2, were retained. Usually, LSQ decreases with the additional step. At the same time, the degree of freedom is reduced by the number of additional parameters, so that $LSQ_1 > LSQ_2$ and $f_1 > f_2$ are valid. In the numerator of Eq. (15), the variance is the difference in the corresponding LSQ_j divided by the difference in the degrees of freedom.

$$F_{exp}=\frac{(LSQ_1-LSQ_2)/(f_1-f_2)}{LSQ_1/f_1} \tag{15}$$

If $F_{exp} > F_{crit}$, model 2 with the variance, V_2 is significantly better suited for the characterization of the measurement than model 1 with the variance, V_1.

Appendix 3

With the Ozawa, Flynn and Wall method [21–23], advantage is taken of the fact that, with increasing heating rate, thermogravimetric measurements shift to higher temperatures. For the same relative mass losses, α_j, the plot of the logarithm of the heating rate, $\ln ß_m$, as a function of the reciprocal temperature, $1/T_{j,m}$, is a line, whose slope is proportional to the activation energy.

For the realization of this method, the TG signal is first transformed into the conversion variable, α: Eq. (16).

$$\alpha_j=\frac{m(t_{m,s})-m(t_{m,j})}{m(t_{m,s})-m(t_{m,f})} \tag{16}$$

where $m(t_{m,s})$ mass at the beginning of the decomposition step,
$m(t_{m,f})$ mass at the end of the decomposition step,
$m(t_{m,j})$ mass at time, $t_{m,j}$, at temperature, $T_{m,j}$.

The equation for the resulting line is Eq. (17):

$$\ln\beta_m=\ln\left(\frac{AE_j}{R}\right)-\ln G(\alpha_j)-5.3305-1.052\frac{E_j}{RT_{m,j}} \tag{17}$$

Since the second term on the right side of Eq. (17) is a constant for constant α_j and the first term is small as compared to the last term, the slope, l, of the resulting line (Fig. 8) is described by $l = -1.052\,E/R$. In order to obtain more exact values for the activation energy, a correction is carried out with respect to $E/RT_{m,j}$ [23].

By averaging over all heating rates applied, β_m, Eq. 18 yields the values for $\ln A$, where E and α_j are known and a first-order reaction is assumed for $G(x) = -\ln(1-\alpha)$.

$$\ln A_j = \ln(-\ln(1-\alpha_j)) - \ln\frac{E_j}{R} + \ln\beta_m - \ln p(z_{m,j}) \quad (18)$$

$$p(z_{m,j}) = \frac{\exp(-z_{m,j})}{z_{m,j}} - \int_{-\infty}^{z_{m,j}} \frac{\exp(-s)}{s}\mathrm{d}s \quad (19)$$

$$z_{m,j} = \frac{E}{RT_{m,j}}$$

If a one-step reaction is now present, the activation energy is independent of the conversion variable x and a horizontal line. Conversely, the dependence of the activation energy on the conversion variable is an indication of the presence of a multiple-step reaction.

* * *

I would like to thank Mr. E. Kaisersberger for various discussions, which contributed greatly to greater clarity.

References

1 H. Mauser, Formale Kinetik, Bertelsmann Universitätsverlag.
2 H. J. Flammersheim, N. Eckardt and J. Opfermann, Thermochim. Acta, 229 (1993) 281.
3 J. Málek, J. Šesták, F. Rouquerol, J. Rouquerol, J. Criado and A. Ortega, J. Thermal Anal., 38 (1992) 71.
4 M. Maciejewski, J. Thermal Anal., 38 (1992) 51.
5 J. Opfermann, G. Wilke, W. Ludwig, S. Hagen, M. Gebhardt and E. Kaisersberger in Thermische Analyseverfahren in Industrie und Forschung, VI. Herbstschule, Meisdorf 14–18. Nov. 1988, Friedrich-Schiller-Universität 1991, ISBN 3-86007-018-5.
6 M. E. Brown, Introduction to Thermal Analysis, Techniques and Applications, Chapman and Hall, London, New York 1989.
7 M. E. Brown, D. Dollimore and A. K. Galwey in Comprehensive Chemical Kinetics, Vol. 22, Reactions in Solid State, ed. C. H. Bamford and C. F. Tipper, Amsterdam 1980, p. 57.
8 A. I. Lesnikovich and S. V. Levchik, J. Thermal Anal., 27 (1983) 85.
9 A. I. Lesnikovich, S. V. Levchik and V. S. Guslev, Thermochim. Acta, 77 (1984) 357.
10 S. Bourbigot, R. Delobel, M. Le Bras and D. Normand, J. Chim. Phys., 90 (1993) 1909.
11 E. Kaisersberger and J. Opfermann, Thermochim. Acta, 187 (1991) 151.
12 E. Kaisersberger and J. Opfermann, Laborpraxis, 4 (1992) 360.
13 J. Opfermann, Proceedings of ESTAC 6, Grado /Italy, p. 219.
14 J. Opfermann, F. Giblin, J. Mayer and E. Kaisersberger: American Laboratory, Febr. 1995, 34.
15 G. Pokol, S. Gál and E. Pungor, Anal. Chim. Acta, 175 (1985) 289.
16 J. P. Elder, Thermochim. Acta, 95 (1985) 41.
17 J. M. Criado and A. Ortega, J. Thermal Anal., 29 (1984) 1075.
18 M. E. Brown, J. Thermal Anal., 49 (1997) 17.
19 J. M. Criado, A. Ortega and F. Gotor, Thermochim. Acta, 157 (1990) 171.
20 J. Madarász, G. Pokol and S. Gál, Proceedings of ESTAC 6, Grado /Italy, p. 180.
21 T. Ozawa, Bull. Chem. Soc. Japan, 38 (1965) 1881.
22 J. Flynn and L. A. Wall, Polym. Lett., 4 (1966) 232.

23 J. Opfermann and E. Kaisersberger, Thermochim. Acta, 11 (1992) 167.
24 J. Šesták, Thermophysical Properties of Solids, Academia, Prag 1984.
25 S. D. Christian and E. R. Tucker, Internat. Laboratory, March 1984, p. 10.
26 H. J. Flammersheim, private communication.
27 G. Engeln-Müllges and F. Reuter, Formelsammlung zur Numerischen Mathematik, Bibliographisches Institut & F. A. Brockhaus AG, Mannheim 1991, ISBN 3-411-15003-3.
28 J. Opfermann, Rechentechnik/Datenverarbeitung 22.3 (1985) 26.
29 J. Opfermann, Manual of the Program NETZSCH Thermokinetics, Version 1998.
30 D. Rasch, G. Herrendörfer, J. Bock and K. Busch, Verfahrensbibliothek – Versuchsplanung und Auswertung, VEB Deutscher Verlag Landwirtschaftsverlag Berlin, Berlin 1981, p. 1105.
31 H.-W. Jank and A. Meister, Kulturpflanze, 30 (1982) 30.
32 J. Opfermann, J. Therm. Anal. Cal., in preparation.